

Evidence for Statistical Equilibrium of the Fragment Isobaric Distributions in Strongly Damped Collisions of ^{86}Kr with ^{166}Er

Y. Eyal

Weizmann Institute of Science, Rehovot, Israel

and

G. Rudolf

Centre de Recherches Nucléaires, Strasbourg, France

and

I. Rode and H. Stelzer

Gesellschaft für Schwerionenforschung, Darmstadt, W. Germany

(Received 29 January 1979)

Primary (pre-evaporation) fragment mass distributions and fragment charge distributions have been measured for deep inelastic collisions of ^{86}Kr with ^{166}Er at $E_{\text{c.m.}} \sim 400$ MeV. It is shown that the relations between the lower moments of the above fragment distributions are consistent with the formation of a statistically equilibrated intermediate dinuclear complex over a wide range of kinetic-energy damping.

A recent study of neutron emission associated with deep inelastic collisions of ^{86}Kr with ^{166}Er has shown that the excitation energy is shared between the fragments in proportion to their mass, indicating that equilibration of the excitation energy in the composite system is achieved during the collision time.¹ An important question is whether the fragment isobaric distributions of strongly damped heavy-ion reactions are also consistent with the equilibration of the intermediate dinuclear complex. Previous investigations of Ar-, Ca-, and Xe-induced reactions, which reported a tendency of the systems to approach N/Z equilibration,²⁻⁴ did not provide a quantitative answer to the above question. In particular, these measurements involved the determination of the final masses and atomic numbers of the fragments. Thus, the observed N/Z values of the products deviated from those of the primary fragments due to neutron and charged-particle emission. In this Letter we present a first comparison between the primary mass and charge distributions, measured for deep inelastic collisions of ^{86}Kr with ^{166}Er at $E_{\text{c.m.}} \sim 400$ MeV. We show that the relations between the lower moments of these distributions agree with those expected from statistical equilibrium according to phase-space considerations over a wide range of total kinetic-energy ($E_{K \text{ tot}}$) loss.

Two separate measurements were performed. Both involved ^{86}Kr beams, provided by the UNILAC accelerator at Gesellschaft für Schwerionenforschung, and 100–250 $\mu\text{g}/\text{cm}^2$ ^{166}Er targets. In the first measurement ($E_{\text{lab}} = 602$ MeV) the primary mass distribution of the fragments was de-

termined. In the second measurement ($E_{\text{lab}} = 616$ MeV) the atomic numbers of the fragments were identified. The small difference between the two bombarding energies is believed to have a negligible influence on the conclusions due to the expected small variation of the cross sections in this energy region.

In the first experiment¹ both fragments were detected in coincidence with the aid of a pair of two-dimensional position-sensitive parallel-plate avalanche counters.⁵ The primary masses and kinetic energies of the fragments, as well as their cross section in the c.m. frame, were computed event by event⁵ from their measured scattering angles and velocities. The experimental resolution, as measured by the width of the elastic peak, was 6 amu [full width at half maximum (FWHM)] in mass and 35 MeV (FWHM) in c.m. $E_{K \text{ tot}}$ of the outgoing fragments. The additional broadening of the observed mass and kinetic-energy distributions due to in-flight particle emission (mainly neutrons) was determined from evaporation calculations⁶ which reproduce the neutron data measured in the same experiment.¹ The uncertainty in the mass determination due to particle emission varies from 4 ± 1 amu (FWHM) at $E_{K \text{ tot}} = 312$ MeV to 7.5 ± 1.5 amu (FWHM) at $E_{K \text{ tot}} = 186$ MeV. The corresponding uncertainties in the observed $E_{K \text{ tot}}$ are 17 ± 5 and 25 ± 5 MeV (FWHM), respectively.

In the second measurement a two-dimensional position-sensitive ionization chamber⁷ was employed to measure the specific ionization (dE/dx) and the kinetic energies of the fragments in a singles mode. Adjacent values of Z were re-

solved for $Z \leq 36$. Further details about the measurement and analysis can be found in Rudolf *et al.*⁸ The observed Z distributions represent very accurately the primary charge distributions. Evaporation calculations^{1,6} indicate that the average value of the charge evaporated is less than 0.4 charge units per fragment even at the highest excitation energies observed in this work. In both measurements the absolute values of the cross sections were obtained by normalization of the elastic yields to Rutherford scattering at small angles.

The experimental cross sections measured in the first experiment are displayed in Fig. 1. The uncertainty in the absolute scale is estimated to be $\pm 20\%$. All angular distributions are forward peaked. However, the angular distributions for completely damped events with nearly symmetric mass division are not very different in shape from a $1/\sin\theta$ curve. This behavior suggests the possible importance of a fusion-fission component. The angular distributions obtained by the Z -identification method exhibit similar features. The two sets of data overlap in the angular ranges $\sim 40^\circ$ – 90° (c.m.) for $E_{K \text{ tot}} \leq 290$ MeV and $\sim 40^\circ$ – 64° c.m. for $E_{K \text{ tot}} > 290$ MeV. By integration of the triple-differential cross section over these angular ranges (missing data points were ob-

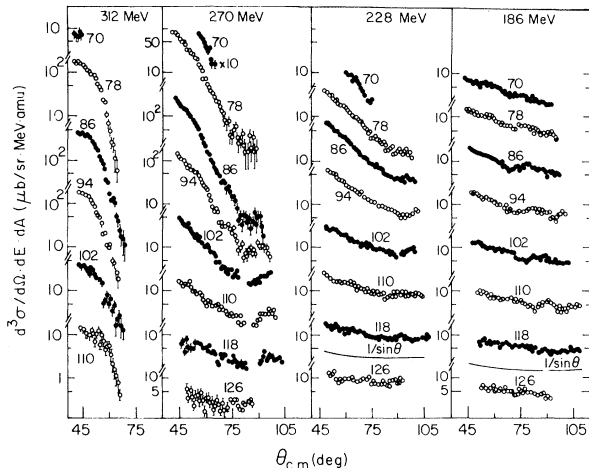


FIG. 1. Experimental fragment–primary-mass differential cross sections at four $E_{K \text{ tot}}$ intervals (312, 270, 228, and 186 MeV) as functions of the c.m. scattering angle of the light fragment, measured for the reaction ^{86}Kr with ^{166}Er at $E_{c.m.} = 396$ MeV. The cross sections are centered around the mass numbers of the light fragments and the $E_{K \text{ tot}}$ values indicated and averaged over intervals of 8 amu in mass and 42 MeV (c.m.) in $E_{K \text{ tot}}$. Included for comparison are two $1/\sin\theta$ curves.

tained by extrapolation according to the trends of adjacent angular distributions), the fragment-mass and -charge distributions in Fig. 2 were obtained.

A comparison is made in Fig. 2 between the fragment–primary-mass and -charge distributions by scaling the mass distribution at $E_{K \text{ tot}} = 228$ MeV to a corresponding Z distribution. A simple transformation was applied: $Z_L = (Z/A)A_L$ and $d^2\sigma/dE dZ = (A/Z)d^2\sigma/dE dA$. Here Z_L and A_L are the atomic and mass numbers, respectively, of the light fragment. The quantity A/Z is the mass-to-charge ratio of the composite system.

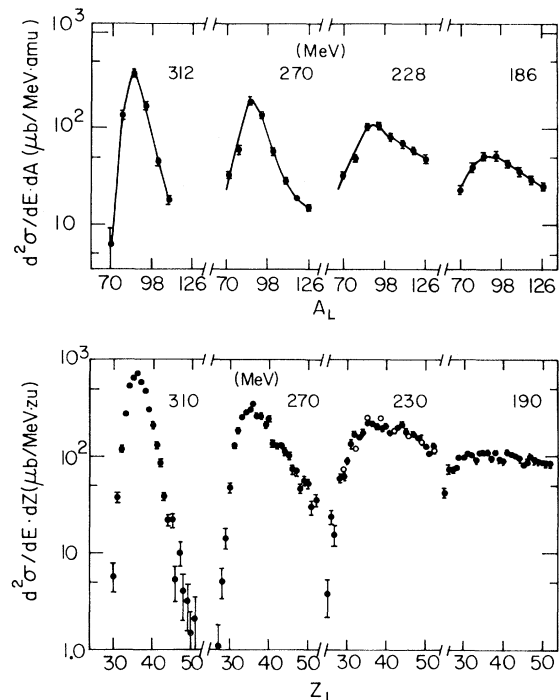


FIG. 2. Upper portion: Angle-integrated (see text) fragment–primary-mass distributions at four $E_{K \text{ tot}}$ intervals (312, 270, 228, and 186 MeV) as functions of the primary mass of the light fragment, A_L , measured for the reaction ^{86}Kr with ^{166}Er at $E_{c.m.} = 396$ MeV. The cross sections are averaged over intervals of 8 amu in mass and 42 MeV c.m. in $E_{K \text{ tot}}$. Lower portion: Angle-integrated fragment-charge distributions at four $E_{K \text{ tot}}$ intervals (310, 270, 230, and 190 MeV) as functions of the atomic number of the light fragment, Z_L , measured for the reaction ^{86}Kr with ^{166}Er at $E_{c.m.} = 405$ MeV. The cross sections are averaged over intervals of 1 charge unit and 20 MeV (c.m.) in $E_{K \text{ tot}}$. The center values of the $E_{K \text{ tot}}$ intervals are indicated. The open circles near the fragment-charge distribution at $E_{K \text{ tot}} = 230$ MeV (lower portion) represent cross section obtained by scaling the fragment-mass distribution at $E_{K \text{ tot}} = 228$ MeV (upper portion) as explained in the text.

The transformation agrees with the prescription of N/Z equilibration. We first note the very good agreement between the absolute values of the scaled cross sections and those of the measured Z distribution at $E_{K \text{ tot}} = 230$ MeV. Secondly, it is clear that the lower moments of the two distributions nearly coincide. We computed the first and second moments of the distributions in Fig. 2, corrected for the experimental mass and charge resolution and for the dispersions associated with particle evaporation. For the ratios between the first moments of the primary-mass and charge distributions we obtain $\langle A_L \rangle / \langle Z_L \rangle = 2.41 \pm 0.03$ over the entire range of $E_{K \text{ tot}}$. The ratios between the second moments of the mass and charge distributions, σ_A^2 / σ_Z^2 , are displayed in Fig. 3.

The observed σ_A^2 / σ_Z^2 values are compared in Fig. 3 with three predictions. The open circles are the results obtained for thermalized intermediate dinuclear complexes, assuming that the isobaric cross sections are proportional to the available density of states in the exit channels. The input parameters for this calculation were the empirical mass distribution and the products of the state densities of all pairs of primary reaction fragments, approximated by a simple Fermi-gas formula, $\exp[2(aE_{\text{ex}})^{1/2}]$. Here $E_{\text{ex}} = E_{\text{c.m.}} - E_{K \text{ tot}} + Q_{\text{gg}} - \delta$ is the effective excitation energy of the composite system, where Q_{gg} is the ground-state Q value of the reaction and δ is the sum of the neutron and proton pairing energies of the fragments taken from Ref. 9. The quantity a is the level-density parameter of the composite sys-

tem and its value was taken as $a = 252/8$. This simple model ignores the dependence of E_{ex} on deformation and rotation. It also neglects the density of momentum states associated with the finite kinetic energy of the fragments at the moment of separation. It is believed that the omission of the above degrees of freedom does not alter considerably the details of the fragment *isobaric* distributions. For the ratios between the first moments of the primary-mass and charge distributions we obtain values within the range $\langle A_L \rangle / \langle Z_L \rangle = 2.35 \pm 0.03$ for all values of $E_{K \text{ tot}}$. The computed values are largely insensitive to variations of the parameter a .

It is evident from Fig. 3 that our results are consistent with a reaction which proceeds through the formation and decay of an equilibrated dinuclear complex. Moreover, because of the large gradients of the potential already at points slightly removed from the most favorable N/Z configuration, the measured σ_A^2 / σ_Z^2 ratios also essentially coincide with the value $(A/Z)^2$, predicted for fully correlated exchange of mass and charge during the collision. The correlation coefficient between neutron and proton exchange, ρ , is defined by $\sigma_A^2 = \sigma_N^2 + \sigma_Z^2 + 2 \cdot \sigma_N \cdot \sigma_Z \cdot \rho$ with $-1 \leq \rho \leq 1$. If the neutron-to-proton ratio of each fragment is exactly equal to the equilibrated N/Z value, then $\sigma_N / \sigma_Z = N/Z$, $\rho = 1$, and $\sigma_A^2 = (A/Z)^2 \sigma_Z^2$. If, on the other hand, the correlation coefficient $\rho = 0$, and nucleon exchange is approximated by a random-walk process with similar neutron- and proton-exchange rates ($\sigma_N^2 / \sigma_Z^2 = N/Z$), the expression $\sigma_A^2 = (A/Z) \sigma_Z^2$ holds. It is seen in Fig. 3 that the latter result largely deviates from our data. Nevertheless, a certain degree of deviation from the relation $\sigma_A^2 = (A/Z)^2 \sigma_Z^2$ can be expected at the early stage of the nucleon-exchange process.

In summary, a comparison between the absolute cross sections and the lower moments of the fragment-primary-mass and -charge distributions, measured for strongly damped collisions of ^{86}Kr with ^{166}Er , shows that the reaction is consistent with the formation of a statistically equilibrated intermediate dinuclear complex. Our results are also consistent with a reaction mechanism in which the exchange of neutrons and protons is highly correlated.

We would like to thank Dr. Z. Artstein, Dr. Z. Fraenkel, Dr. J. R. Huizenga, and Dr. L. Moretto for valuable discussions. Two of us (Y. E. and G. R.) are greatly indebted to Dr. R. Bock, Dr. A. Gobbi, and Dr. U. Lynen for many helpful sug-

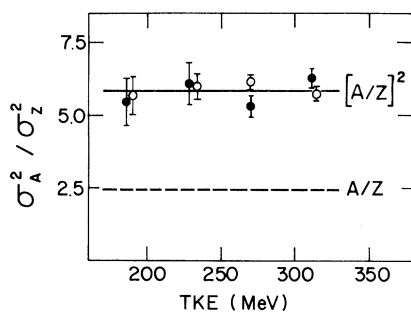


FIG. 3. Ratio between the second moment of the fragment-primary-mass distribution, σ_A^2 , and the second moment of the fragment-charge distribution, σ_Z^2 , as function of total kinetic energy, measured for the reaction ^{86}Kr with ^{166}Er at $E_{\text{c.m.}} \sim 400$ MeV (filled circles). The open circles are the results of a calculation which assumes the existence of an equilibrated intermediate complex (see text). The quantity $A/Z (= 2.42)$ is the mass-to-charge ratio of the composite system.

gestions and for their warm hospitality during their stay at Darmstadt.

¹Y. Eyal *et al.*, Phys. Rev. Lett. **41**, 625 (1978).

²B. Gatty *et al.*, Z. Phys. **A273**, 65 (1975); B. Gatty *et al.*, Nucl. Phys. **A253**, 511 (1975).

³J. V. Kratz *et al.*, Phys. Rev. Lett. **39**, 984 (1977).

⁴J. Barrette *et al.*, Nucl. Phys. **A299**, 147 (1978);

P. Braun-Munzinger and J. Barrette, Nucl. Phys. **A299**, 161 (1978).

⁵Y. Eyal and H. Stelzer, Nucl. Instrum. Methods **155**, 157 (1978).

⁶M. Hillman and Y. Eyal, code JULIAN (unpublished).

⁷H. Sann *et al.*, Nucl. Instrum. Methods **124**, 509 (1975).

⁸G. Rudolf, A. Gobbi, H. Stelzer, U. Lynen, A. Olmi, H. Sann, R. G. Stokstad, and D. Pelte, to be published.

⁹A. Gilbert and A. G. W. Cameron, Can. J. Phys. **43**, 1446 (1965).

Coriolis Interaction

A. J. Kreiner

Departamento de Física, Comisión Nacional de la Energía Atómica, 1429 Buenos Aires, Argentina

(Received 17 August 1978)

A possible explanation of the intriguing problem of the so-called Coriolis attenuation factors, in the framework of the particle-plus-rotor model, is suggested. The explicit inclusion of the recoil term renders unnecessary the assumption of an attenuation factor for the Coriolis interaction and leads to a hitherto unsuspected parallelism with the cranking model.

For several years it has been generally accepted^{1,2} that the particle-plus-rotor model² (PRM) is able to reproduce Coriolis-distorted bands quantitatively only if the strength of the Coriolis interaction is considerably reduced; this has remained as an outstanding puzzle in these calculations. In order to compensate for the supposedly too large Coriolis matrix elements purely *ad hoc* attenuation factors have been introduced.¹ It has also been asserted^{3,4} that such a problem does not appear if the cranking model (CM) is applied. In this Letter I show that a complete treatment of the PRM gives indeed a satisfactory answer.

The Hamiltonian to be used is given by²

$$H = (\hbar^2/2\theta)\vec{R}^2 + h_0 \\ = (\hbar^2/2\theta)[I(I+1) - I_3^2 - 2\vec{I}^\perp \cdot \vec{j}^\perp + j^{\perp 2}] + h_0. \quad (1)$$

The superscript \perp denotes those components lying in the plane perpendicular to the symmetry axis. h_0 comprises a one-body operator for the mean field (a Nilsson Hamiltonian) and a two-body term which accounts for the pairing correlations (which has been treated here in the BCS approximation). Recalling that $I_3 = j_3$, Eq. (1) may be rewritten in the following way:

$$H = (\hbar^2/2\theta)[I(I+1) - j^2 - 2\vec{j}^\perp \cdot (\vec{I}^\perp - \vec{j}^\perp)] + h_0. \quad (2)$$

The true Coriolis interaction is

$$H_C = -(\hbar^2/\theta)\vec{j}^\perp \cdot (\vec{I}^\perp - \vec{j}^\perp) \\ = -\hbar\vec{j} \cdot (\hbar\vec{R}/\theta) = -\hbar\vec{j} \cdot \vec{\omega}. \quad (3)$$

Indeed, the field producing the Coriolis effect is the angular velocity associated with the collective rotation and the expectation value of the Coriolis interaction [calculated with the eigenstates of the full Hamiltonian of Eq. (1)] becomes

$$\langle H_C \rangle = -\frac{\hbar^2}{\theta} \langle \vec{j}^\perp \cdot \vec{I}^\perp \rangle \left(1 - \frac{\langle \vec{j}^\perp \cdot \vec{j}^\perp \rangle}{\langle \vec{j}^\perp \cdot \vec{I}^\perp \rangle} \right). \quad (4)$$

As compared to the situation in which the recoil term ($j^{\perp 2}$) is neglected (which amounts to considering the interaction with the total angular momentum rather than R) it is seen that the explicit inclusion of this term naturally leads to an attenuation of the particle-rotation coupling $\langle \vec{j}^\perp \cdot \vec{I}^\perp \rangle$.

As we restrict ourselves to a basis of one-quasiparticle-plus-rotor states for the description of odd- A nuclei, only the one-quasiparticle part of the recoil operator has to be considered. The importance of this term in connection with the location of bandhead energies has already been stressed by Osnes, Rekstad, and Gjøtterud.⁵ Indeed, this term mainly produces a significant renormalization of the single-quasiparticle spectrum thus affecting in a major way the effect of the nondiagonal part of the Coriolis interaction. In cases where the quasiparticle states strongly coupled by the Coriolis interaction have the same high- j unique-parity parentage essentially only H_C (and h_0) determines the wave functions because the j^2 operator is nearly constant.

We come now to the comparison between the